Oxygen isotopic composition of the solar nebula gas inferred from high-precision isotope imaging of melilite crystals in an Allende CAI

Park C., Wakaki S., Sakamoto N., Kobayashi S. and Yurimoto H. (2012)

Meteoritics & Planetary Science 47, pp.2070-2083

1st June 2018 Text seminar

Sohei Wada

Contents

About Melilite

Melilite Åkermanite, $Ca_2MgSi_2O_7$ — Gehlenite, $Ca_2Al_2SiO_7$ solid solution

One of common primary minerals in CAIs

Formation of normally zoned melilite vs. reversely zoned

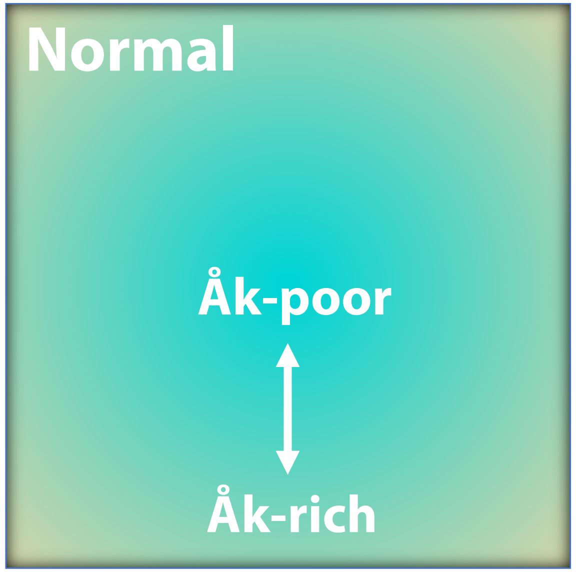

formed by igneous or condensation processes (Grossman 1972)

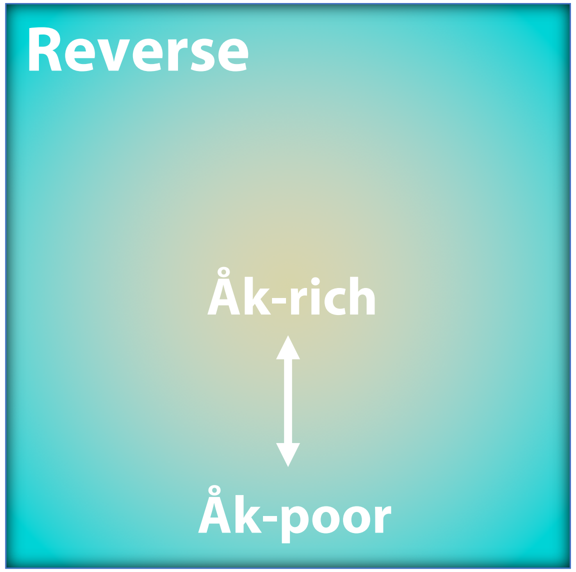

formed by condensation from gas (MacPherson and Grossman 1984).

Reversely zoned melilite

Commonly observed in Fluffy Type A CAIs

may have recorded oxygen isotope composition of the solar nebula gas

Various thermal processes in the nebula and on the parent body

Some CAIs may have experienced these processes. The oxygen isotope in CAI melilites may have exchanged with the surrounding gas in the nebula and aqueous fluid on the parent body.

Reversely zoned melilite

Several processes have been proposed to explain the large variations in the O-isotopic compositions of melilite grains.

1. Isotope exchange between the gas and partially molten CAI
2. Gas-solid interaction and solid state diffusion by repetitive heating over a long accumulated time.
3. Isotope exchange with fluid during aqueous alteration and metamorphism on a parent body.

Purpose and Methods

In situ analyses

Since the variations in the O-isotopic compositions are on submicron order, *in situ* analyses are necessary to identify.

Isotope imaging

useful to distinguished the primary and secondary features of the oxygen isotopic compositions (Yurimoto et al. 2003, Kunihiro et al. 2005)

They conducted *in situ* spot analyses and isotope imaging in order to identify whether these processes were existence or not.

Analytical techniques

Petrography

FE-SEM; JEOL JSM-7000F
EDS; Oxford INCA Energy
To obtain BSE images and X-ray maps, and to conduct quantitative chemical analyses

Petrography

EBSD; Oxford Instruments

To determine grain boundaries

In situ analyses

SIMS; Cameca ims-1270

To analyze the O-isotopic compositions on submicron order

Isotope imaging

SIMS; Cameca ims-1270
SCAPS
To obtain quantitative isotope images

Quality of Isotopography

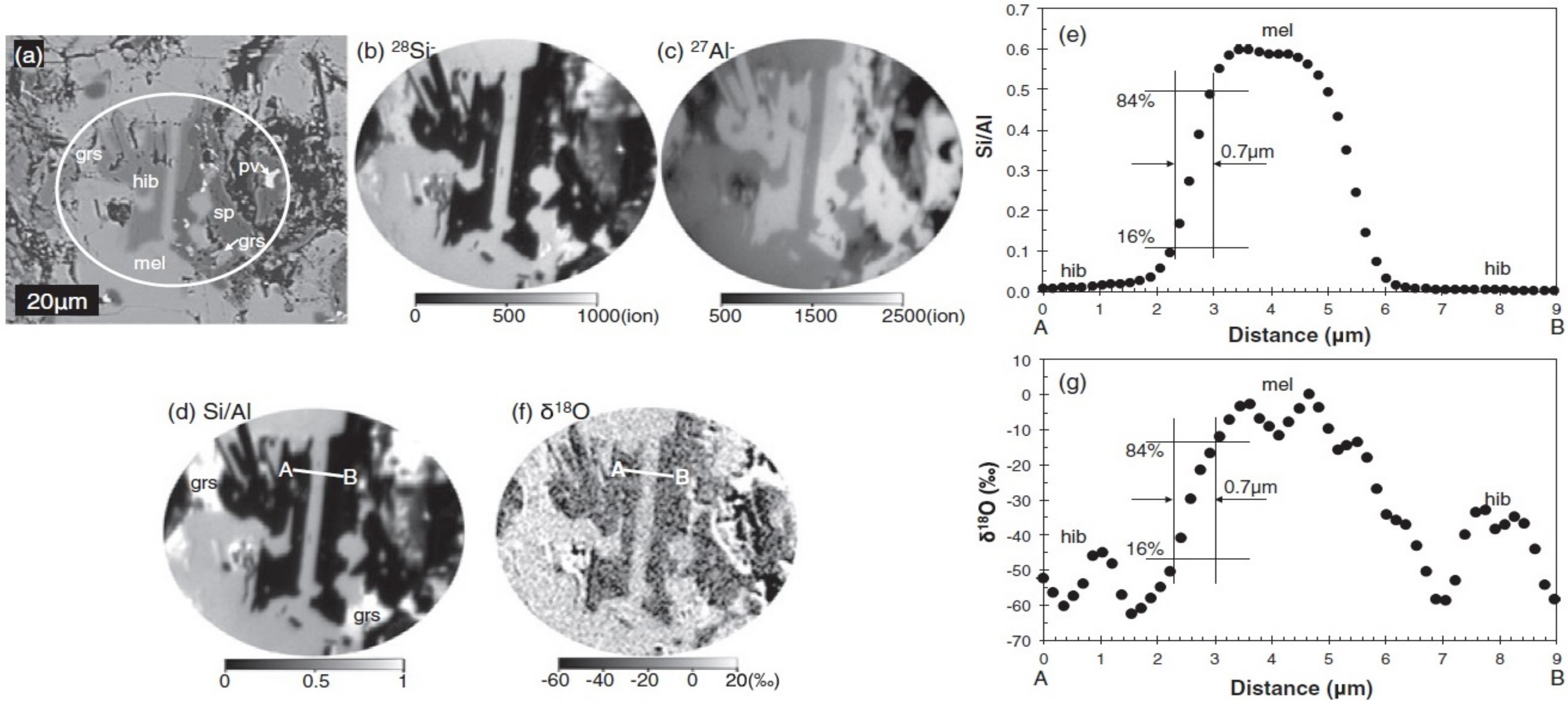

Fig. 2. SEM image, Isotopograph and line profiles from A to B in #1.

Petrography

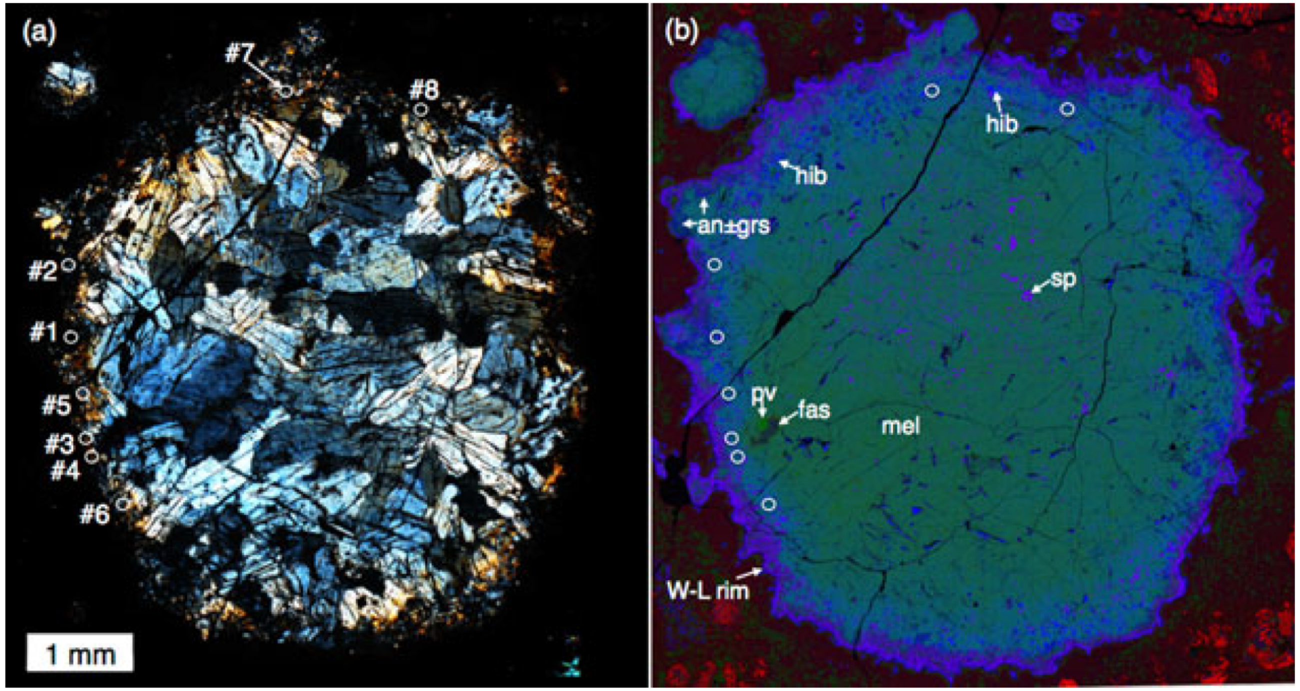

Fig.1 (a) Cross polarized light image

Fig.1 (b) X-ray RGB (**Mg** **Ca** **Al**) map image

Forming minerals

Melilite, few Spinel, Perovskite, Fassaite

Texture

Coarse-grained compact Type A CAI

Åkermanitic core

~100μm grain size, Åk~28

Gehlenitic mantle

<~100μm grain size, Åk~10

O-isotopic composition of mantle melilite

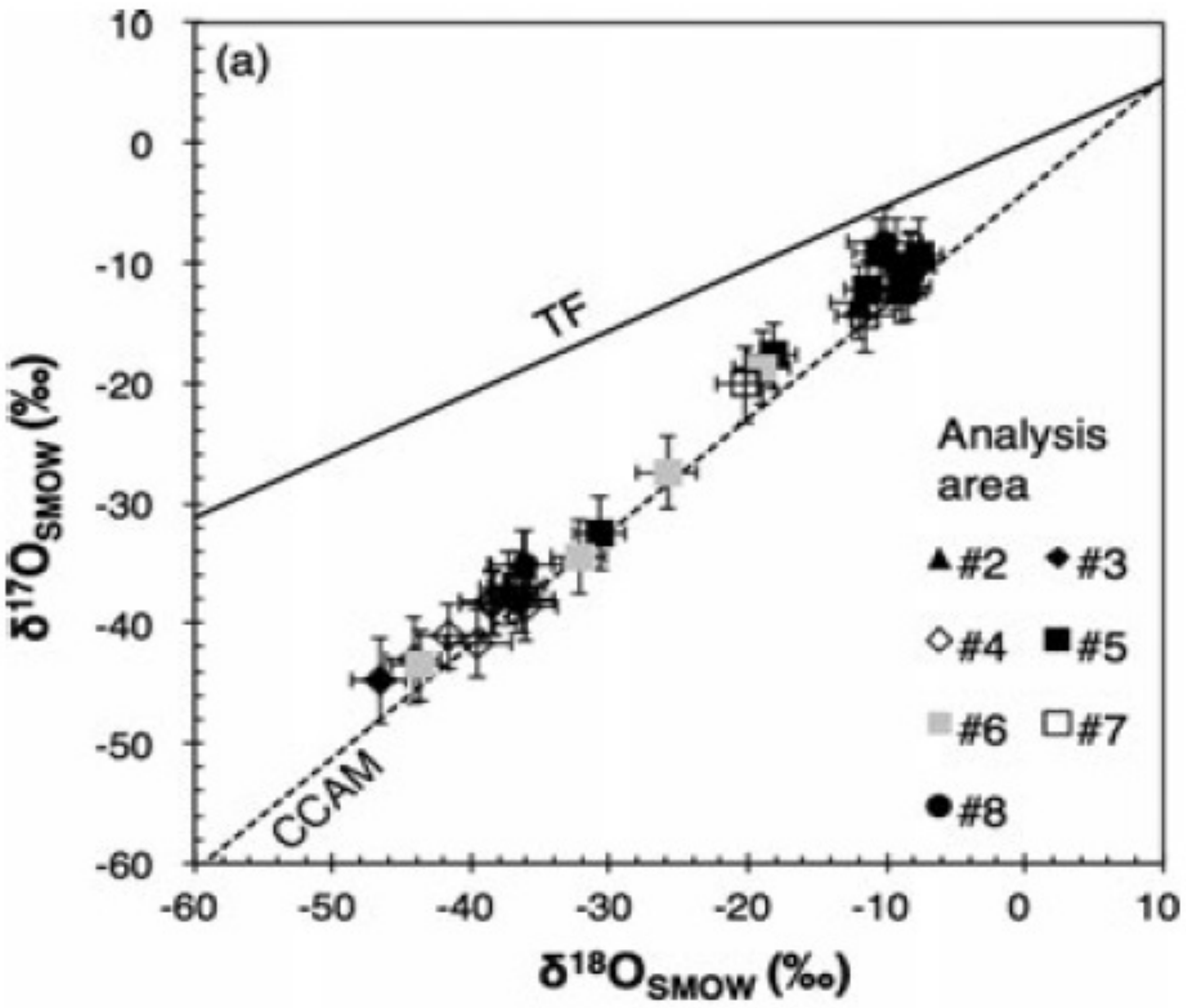

Fig. 3. Oxygen isotopic distribution in mantle melilites.

The O-isotopic composition of melilites in Gehlenitic melilite mantle vary from -45 to -10 ‰ for δ18O.

Imaging

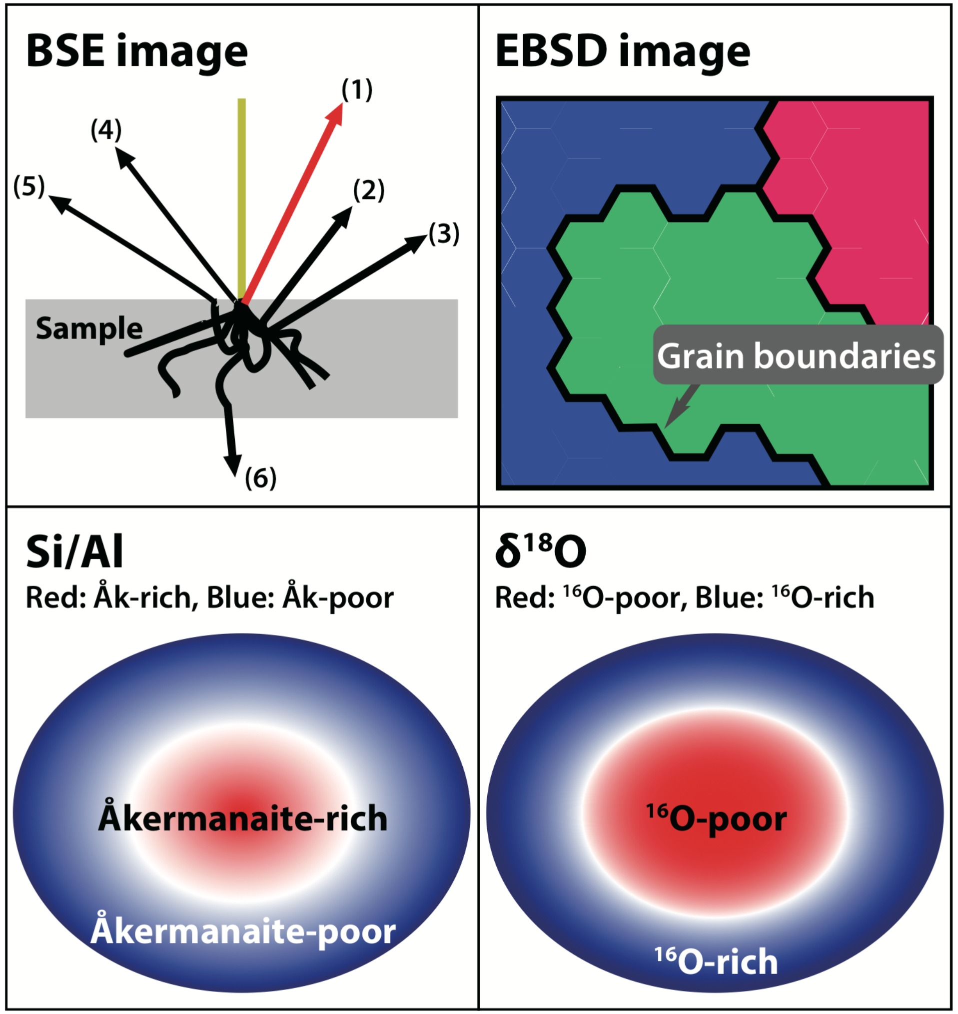

Schematic diagram

BSE image

(1) Back scattered electron

EBSD image

The difference in color reflects the difference in crystal direction.

Si/Al

Red: Åk-rich, Blue: Åk-poor

$\delta^{18}O$

Red: ^{16}O-poor, Blue: ^{16}O-rich

Isotopography: uniform depletion of ^{16}O

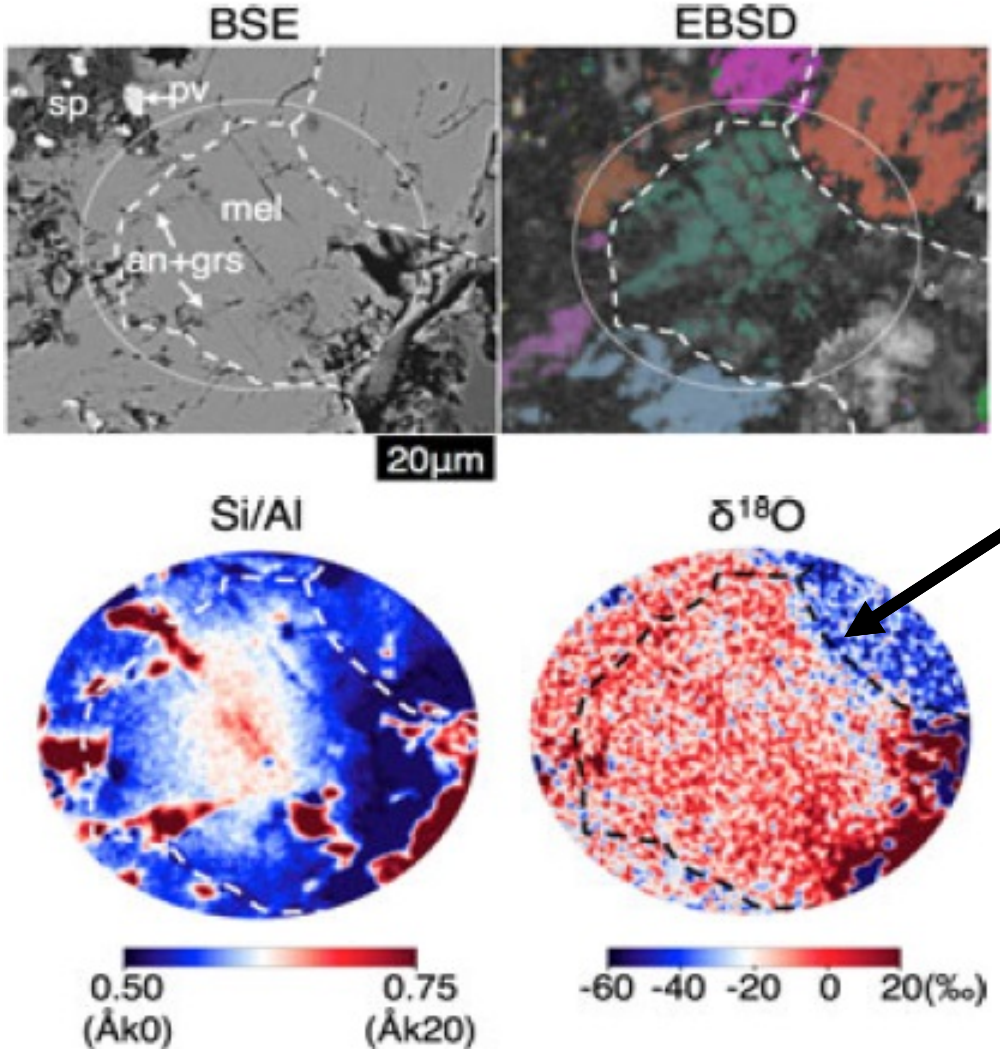

Fig. 4. SEM image and isotopograph of #2.

The strikingly different O-isotopic compositions among the melilite grains can be seen.

Isotopography: uniform enrichment of ^{16}O

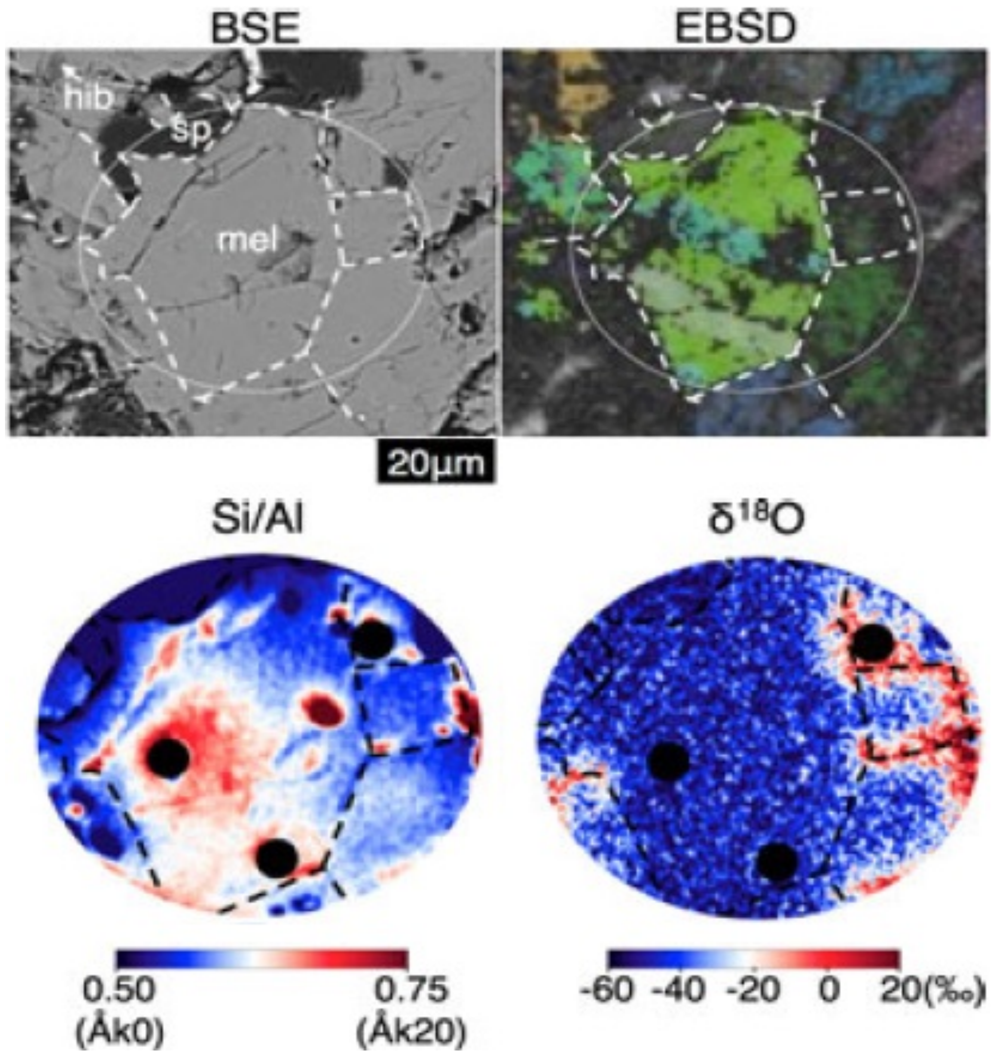

Fig. 5. SEM image and isotopograph of #3.

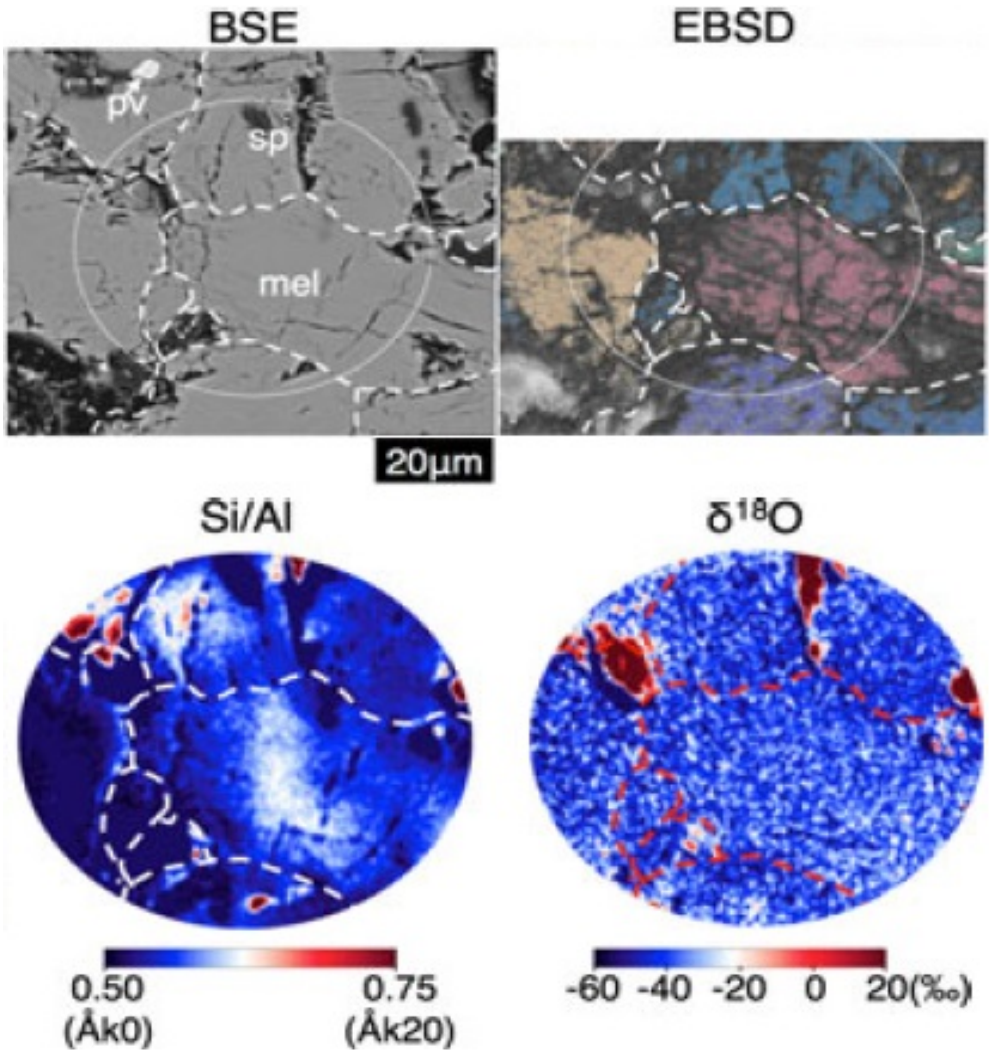

Fig. 6. SEM image and isotopograph of #4.

Isotopography: variation from ^{16}O-poor core to ^{16}O-rich rim

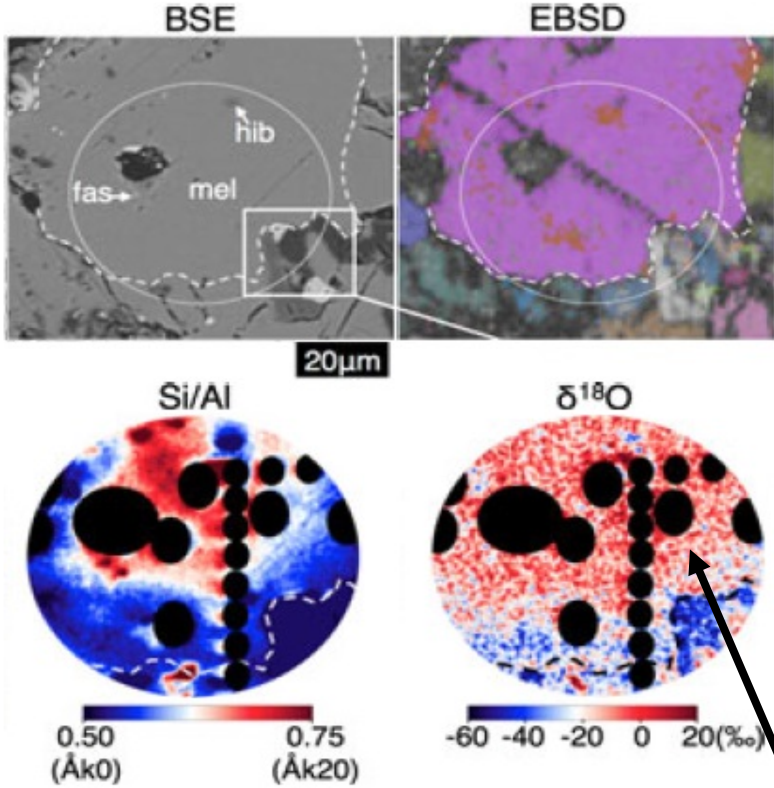

Fig. 7. SEM image and isotopograph of #5.

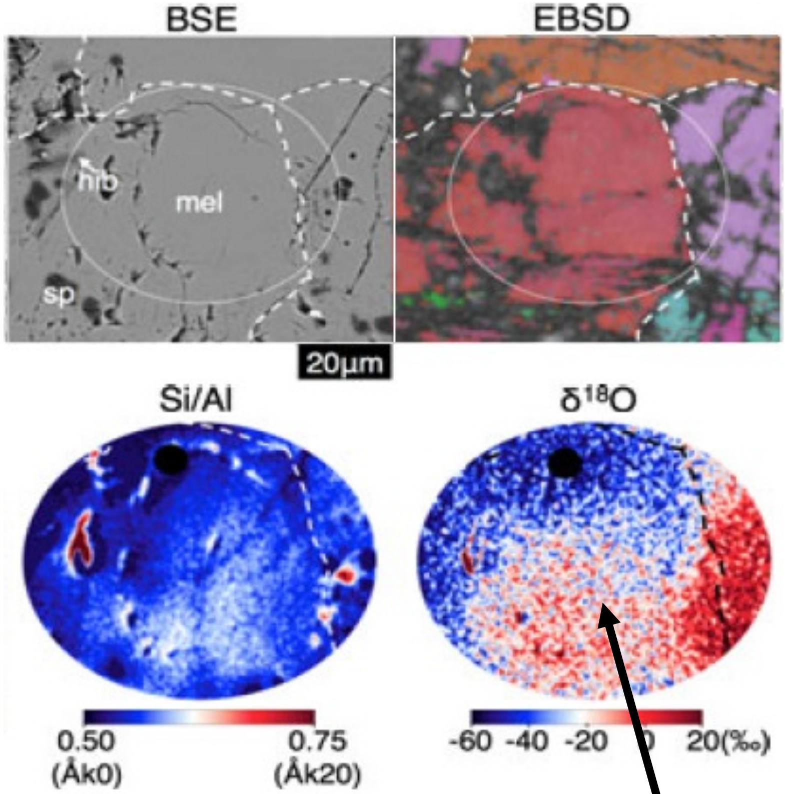

Fig. 8. SEM image and isotopograph of #6.

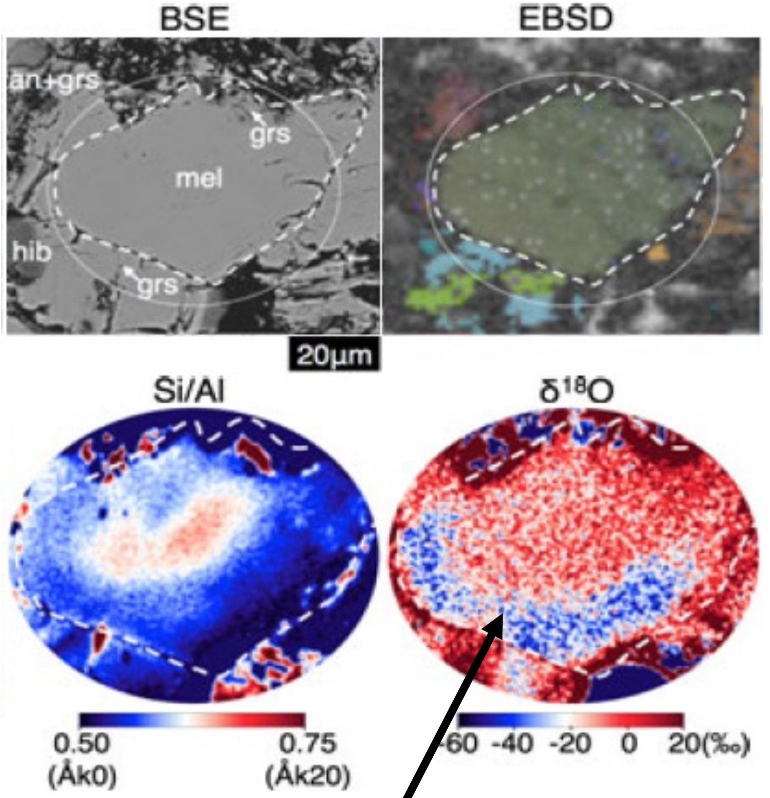

Fig. 9. SEM image and isotopograph of #7.

The wide and gradual change of O isotopes in a single crystal can be seen.

Isotopography: ^{16}O-poor crystal rim

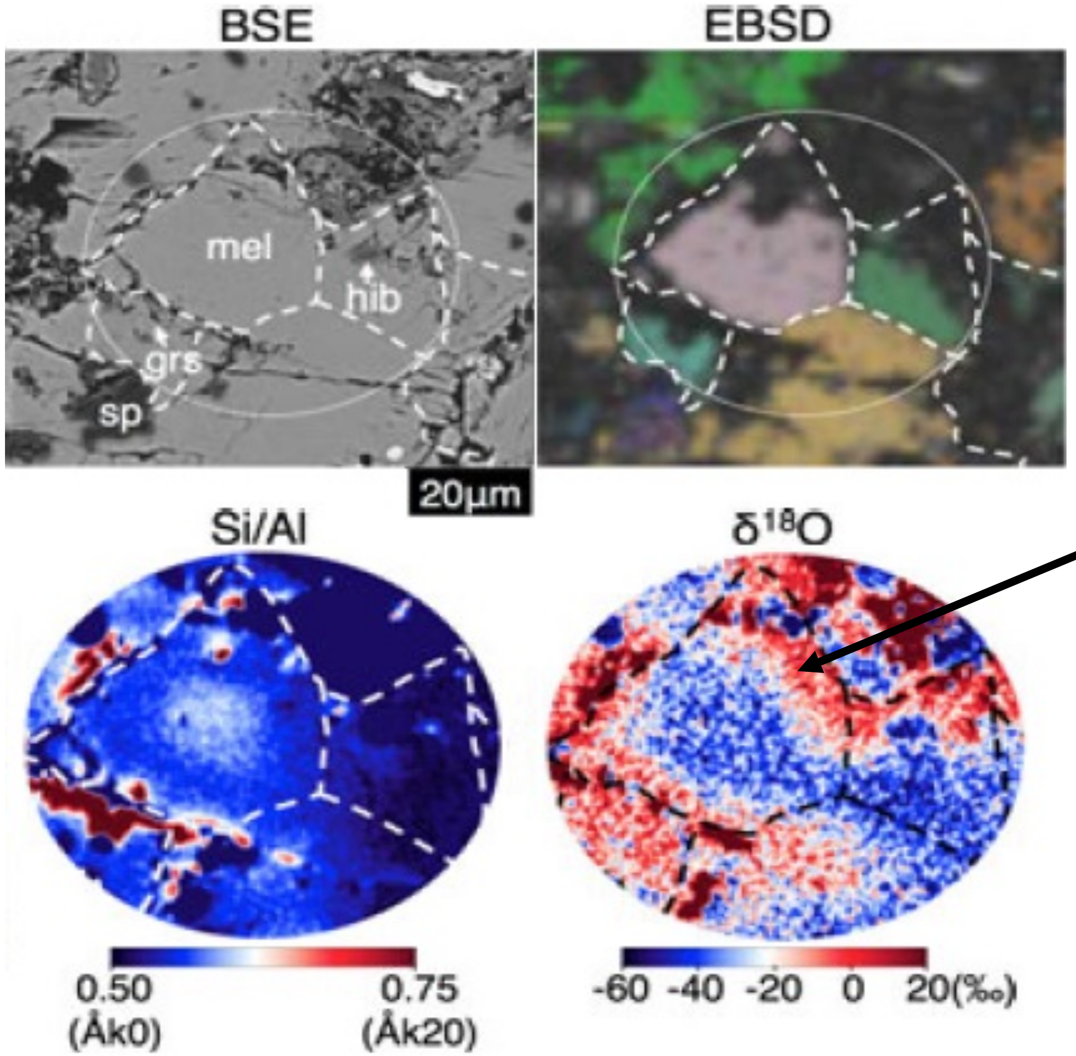

Fig. 10. SEM image and isotopograph of #8.

^{16}O-poor compositions of ~10µm near holes, cracks, or secondary phases can be seen.

Discussion

The formation of reverse zonation throughout melilite crystals is best explained by gas-solid condensation (MacPherson and Grossman 1984).

➡ Reversely zoned melilites should recorded the O-isotopic composition of the solar nebula gas in which the melilites condensed.

However, Oxygen isotopic compositions could have been modified by …

1. **Gas-melt interaction**
2. **Gas–solid diffusive exchange**
3. **Fluid assisted thermal metamorphism**

Gas–melt interaction

Reversely zoned melilites could be formed by igneous process?

Very unlikely to be formed by simple melt-crystallization

If anorthite crystallization is suppressed in the melt with the Type B CAI composition, then pyroxene could be cocrystallized with reversely zoned melilite (MacPherson et al. 1984).

➡ The reverse zoning in Type B significantly different from the observations in this study.

Reversely zoned melilite could be reproduced by evaporation of a melt (Grossman et al. 2002).

➡ Unrealistic

Gas–melt interaction

Different O-isotopic compositions among the melilite grain could be formed from a single melt composition?

Oxygen isotopes in the melt would be quickly homogenized.

The wide and gradual change of oxygen isotopes in a single crystal (Fig. 7-9) is **inconsistent** with the origin from a melt.

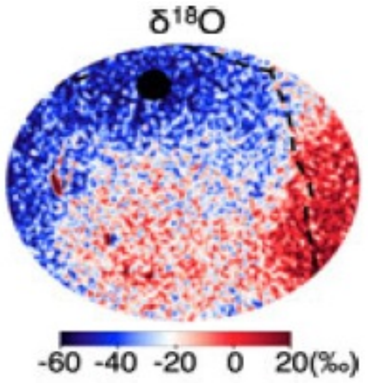

Fig. 8. Isotopograph of #6

Partial melting may result in oxygen isotope variation within a single crystal.

The O-isotopic distribution changes abruptly with in a single crystal

(Yurimoto et al. 1998)

Gas–melt interaction

Therefore, the best explanation for the reverse zoning is direct condensation from a gas.

- **A small degree of pressure decrease could result in the reverse zoning of melilite.**
- **Gas-melt interaction may not have occurred in ON01.**

Gas–solid diffusive exchange

Gradually O-isotope compositional change can be explained by gas-solid interaction followed by solid-state diffusion occurred by **repetitive heating events** at high temperature (Simon et al. 2011).

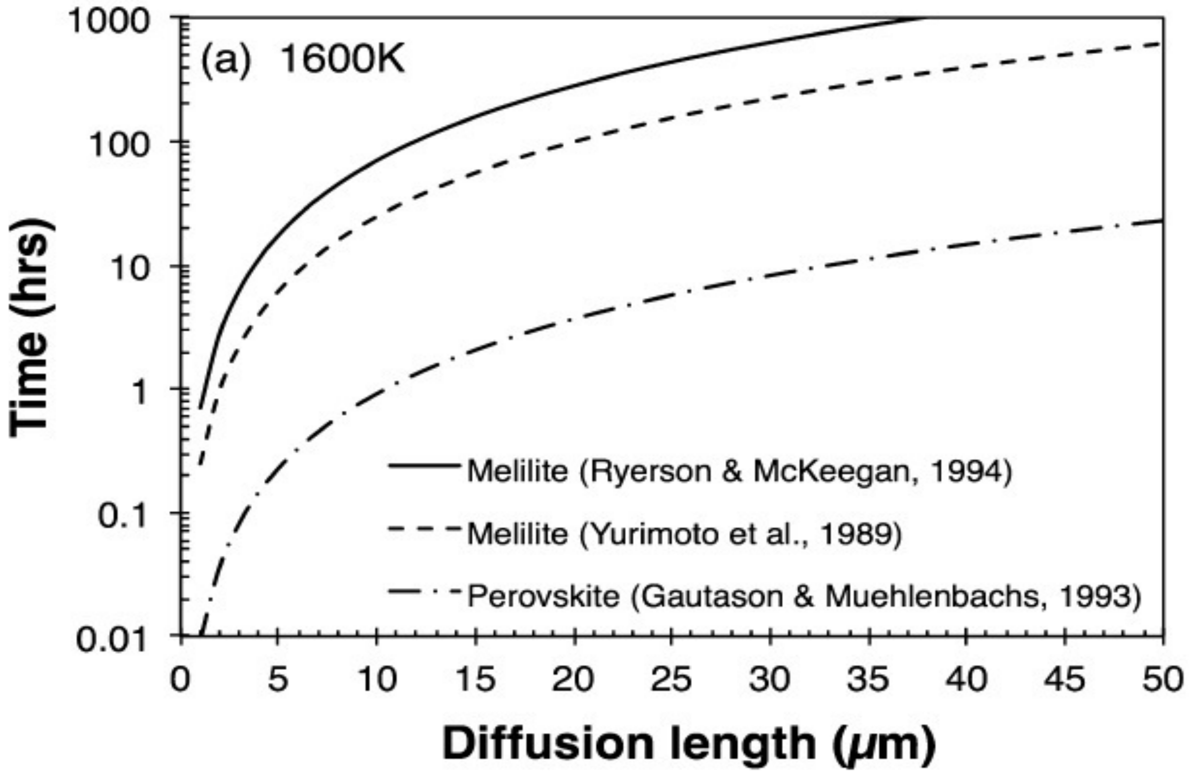

Fig. 11. O-diffusion in melilite and perovskite at 1600K.

The $\delta^{18}O$ values across the grain boundary of melilite (Fig. 4) are inconsistent with this model.

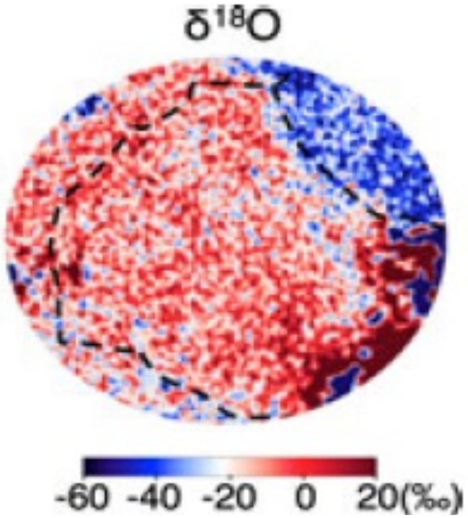

Fig. 4. Isotopograph of #2.

The gas-solid diffusion in the nebula is also excluded.

Fluid-assisted thermal metamorphism

Metamorphism on the Allende parent body

Allende is thought to be one of the most metamorphosed CV3 chondrites (Bonal et al. 2006).

The peak temperature ~800K (Weinbruch et al. 1994).

Generally associated with aqueous alteration (Krot et al. 1998).

This fluid was ^{16}O-poor ($\Delta^{17}O$ ~ -3 - 0‰) (Choi et al. 1997).

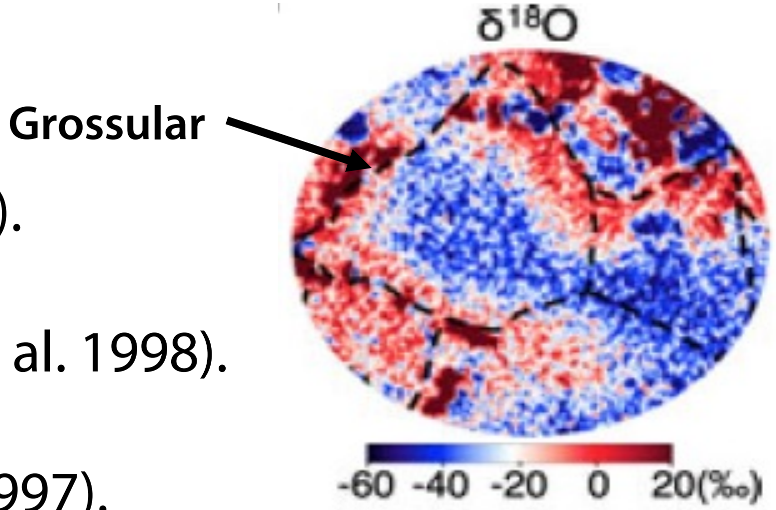

Fig. 10. Isotopograph of #8.

This O-isotopic composition is similar to those of the secondary anorthite and grossular in ON01, implying that **their O-isotopic composition reflect that of the fluid on the CV parent asteroid** (Yurimoto et al. 2008).

Fluid-assisted thermal metamorphism

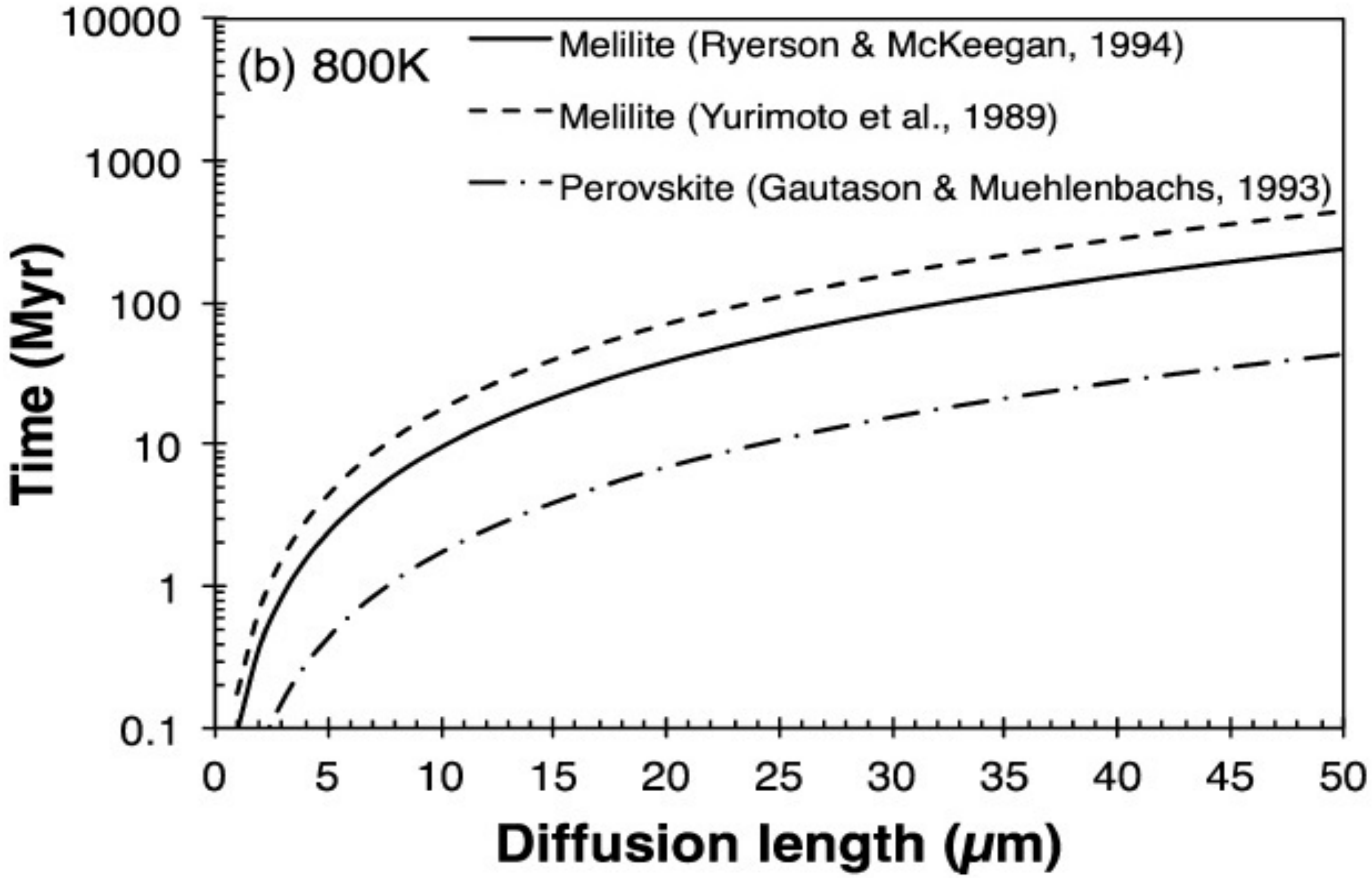

Fig. 12. O-diffusion in melilite and perovskite at 800K.

The O self-diffusion in melilite is extremely slow even at 800K

➡ **Unrealistic** for the thermal history (Weinbruch et al. 1994).

Lattice diffusion becomes faster in the presence of fluid.
(Krot et al. 2008).

➡ The melilites **don't corresponded the concept** of fast oxygen self diffusion.

Fluid-assisted thermal metamorphism

Wasson et al. (2001) suggested alternative idea.

^{16}O-poor areas within ^{16}O-rich melilite reflect alteration of the oxygen isotopes by dissolution and reprecipitation (Nakamura et al. 2005).

However, a reset of oxygen isotopes cannot occur in the core of large melilite.

➡ Cannot be simply explained by aqueous alteration on the parent body.

\+ The parent body process could not lead to change of ^{16}O-poor to ^{16}O-rich.

➡ Only melilite grains with ^{16}O-poor crystal rim may have the result of fluid-assisted thermal metamorphism.

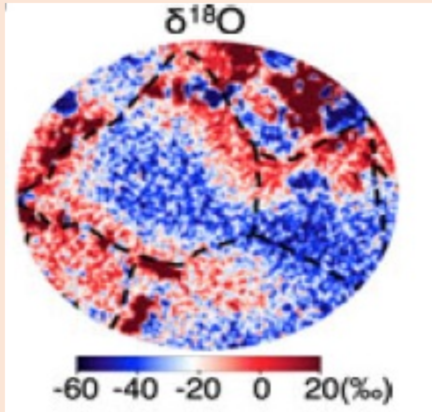

Direct records of gas composition

1. Gas-melt interaction
2. Gas-solid diffusive exchange

➡ **Cannot be explained for the oxygen isotopic variations**

3. Fluid assisted thermal metamorphism

➡ **Could partly disturb the oxygen isotopes**

The three types of oxygen isotopic composition (uniform depletion of ^{16}O, uniform enrichment of ^{16}O and variation from ^{16}O-poor core to ^{16}O-rich rim) directly reflect those of solar nebula gas.

Formation of the Gehlenite mantle

Hypothesis

Reversely zoned melilites in the Gehlenite mantle are evidence for the mantle condensed from gas.

➡ Other minerals in Gehlenite mantle (Hibonite, spinel and perovskite assemblages) should also be formed by condensation.

Texture of the assemblage:

Spinel replaces hibonite

Small perovskite grains are attached to the spinel

Formation of the Gehlenite mantle

Hibonite | Gas | Gas | Gas

$$CaMg_xTi_xAl_{12-2x}O_{19} + (6 - 2x)Mg + (1 - x)TiO_2 + (6 - 2x)H_2O$$

Spinel | Perovskite | Gas

$$\rightarrow (6 - x)MgAl_2O_4 + CaTiO_3 + (6 - 2x)H_2$$

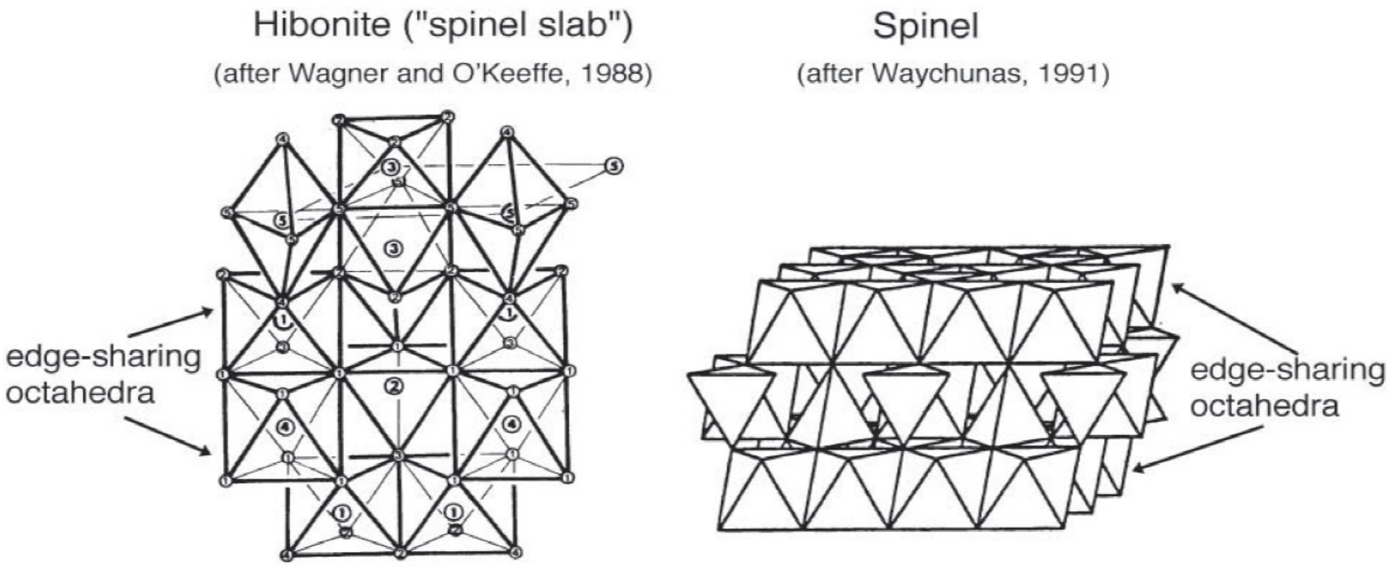

Fig. . Crystal structure of hibonite and spinel (from Simon et al. 2006).

The texture of this mineral assemblage can be explained by condensation.

Formation of the Gehlenite mantle

Hibonite: $CaMg_xTi_xAl_{12-2x}O_{19}$ + Gas: $(6-2x)Mg$ + Gas: $(1-x)TiO_2$ + Gas: $(6-2x)H_2O$

$\rightarrow$ Spinel: $(6-x)MgAl_2O_4$ + Perovskite: $CaTiO_3$ + Gas: $(6-2x)H_2$

The oxygen compositions of spinel and perovskite are inherited from that of the reactant hibonite.

If hibonite is uniformly ^{16}O-enriched ($\delta^{18}O$ ~ -55‰), then spinel and perovskite are also ^{16}O-rich. Spinel and perovskite could have the ^{16}O-rich composition, regardless of the O-isotopic composition of the gas.

Formation of the Gehlenite mantle

Hibonite: $CaMg_xTi_xAl_{12-2x}O_{19}$ + Gas: $(6-2x)Mg$ + Gas: $(1-x)TiO_2$ + Gas: $(6-2x)H_2O$

$\rightarrow$ Spinel: $(6-x)MgAl_2O_4$ + Perovskite: $CaTiO_3$ + Gas: $(6-2x)H_2$

$$CaMg_xTi_xAl_{12-2x}O_{19} + (6-2x)Mg + (1-x)TiO_2 + (6-2x)H_2O \rightarrow (6-x)MgAl_2O_4 + CaTiO_3 + (6-2x)H_2$$

The texture of assemblages can be explained by condensation.
Spinel and perovskite have the ^{16}O-rich compositions, regardless of the O-isotopic composition of the gas.

These conclusions support the hypothesis that reversely zoned melilites in the Gehlenite mantle are evidence for the mantle condensed from gas.

Formation of the Gehlenite mantle

Spinel and perovskite are formed by melt crystallization?

Crystallization sequence from a melt of Type A CAI

Spinel → Gehlenitic melilite → Perovskite

➡ O-isotopic compositions of melilite should be the same as those of spinel and perovskite.

However, ^{16}O-rich spinel and perovskite adjoin ^{16}O-poor melilite.

These minerals were formed by condensation.

Formation of the Gehlenite mantle

The Gehlenite mantle formed by aggregation of gas condensates to pre-existing inclusion

Mechanism

Reversely zoned melilite could have formed by the condensation with a decrease in pressure (MacPherson and Grossman 1984).

+

The solar nebula gas changed from ^{16}O-poor to ^{16}O-rich during the crystal growth of reversely zoned melilite.

Mechanism

Itoh and Yurimoto (2003) proposed likely scenario to explain the coexistence of two oxygen isotopic reservoir.

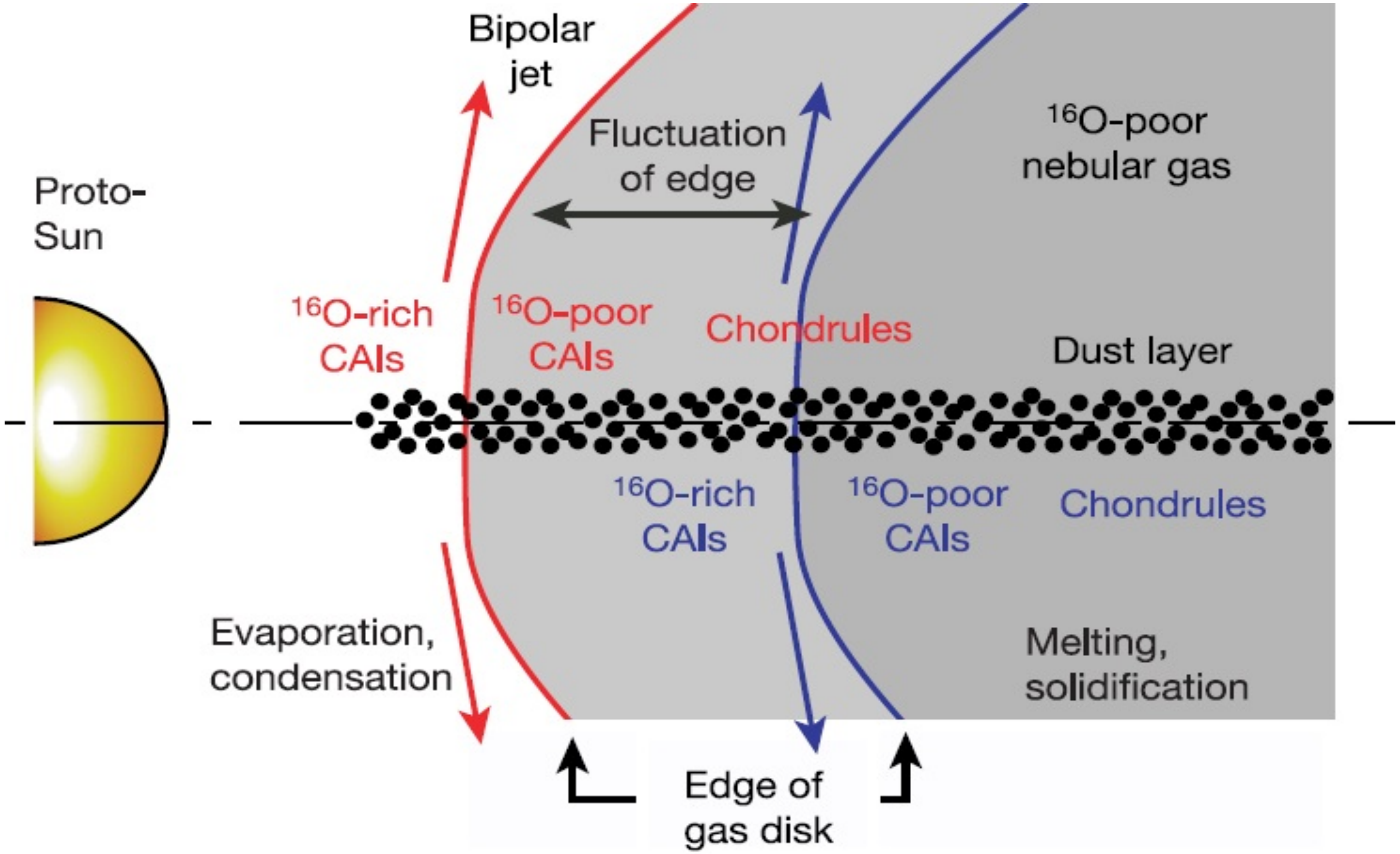

Fig. 15. Schematic view of CAI and chondrule formation (Itoh and Yurimoto 2003).

Mechanism

Reversely zoned melilite

with compositional variation from ^{16}O-poor to ^{16}O-rich could be formed in the fluctuation zone.

with uniformly ^{16}O-enriched or ^{16}O-depleted compositions could have formed in the ^{16}O-rich or ^{16}O-poor gasses when gas pressure decreased.

Conclusion

They conducted *in situ* spot analyses and isotope imaging in order to identify whether secondary processes were existence or not.

The three types of oxygen isotopic composition (uniform depletion of ^{16}O, uniform enrichment of ^{16}O and variation from ^{16}O-poor core to ^{16}O-rich rim) in CTA CAI ON01 from Allende meteorite directly reflect those of solar nebula gas.

Reversely zoned melilites could be formed by condensation in the fluctuation zone of the protoplanetary disk.